Supporting Information

Two new estertin modified tungstosilicates: synthesis, catalytic activity and photoelectrochemical property

Yao Zhang,‡ Meng-Xuan Li,‡ Qiang Hao, Fang Su, Zai-Ming Zhu, Jian-Sheng Li, Xiao-Jing Sang,* Chang-Sheng Wang,* Lan-Cui Zhang*

1. Computational result

2. Crystal structure figures

3. Selected bond lengths and angles

4. Chemical and physical characterizations

1. Computational result

Table S1 The energy level of frontier molecular orbits for $[O_3SnCH_2CH_2COOCH_3]^{3-}$ and **Si_2W_{20}-Co**

	Energy for HOMO	**Energy for LUMO**
$[O_3SnCH_2CH_2COOCH_3]^{3-}$	−4.591 eV	−0.005 eV
Si_2W_{20}-Co	−5.994 eV	−4.324 eV

2. Crystal structure figures

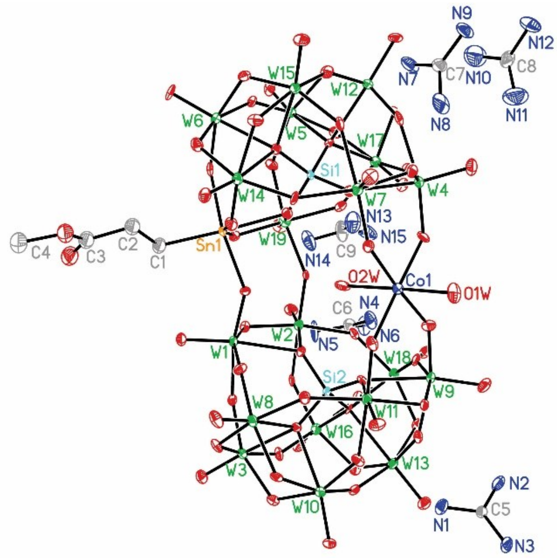

Figure S1 ORTEP drawing of **Si_2W_{19}-Co-SnRCOOCH$_3$** with thermal ellipsoids at 30% probability (All water molecules, K, Na and H atoms were deleted for clarity)

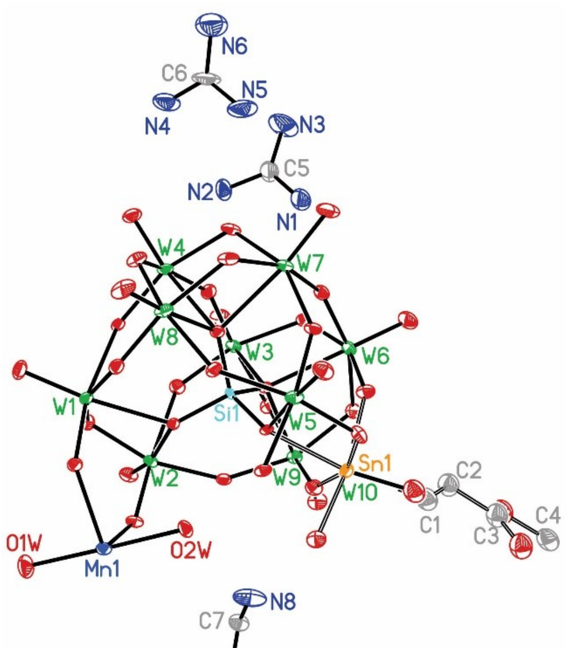

Figure S2 ORTEP drawing of **Si_2W_{19}-Mn-SnRCOOCH$_3$** with thermal ellipsoids at 30% probability (All water molecules, K, Na and H atoms were deleted for clarity)

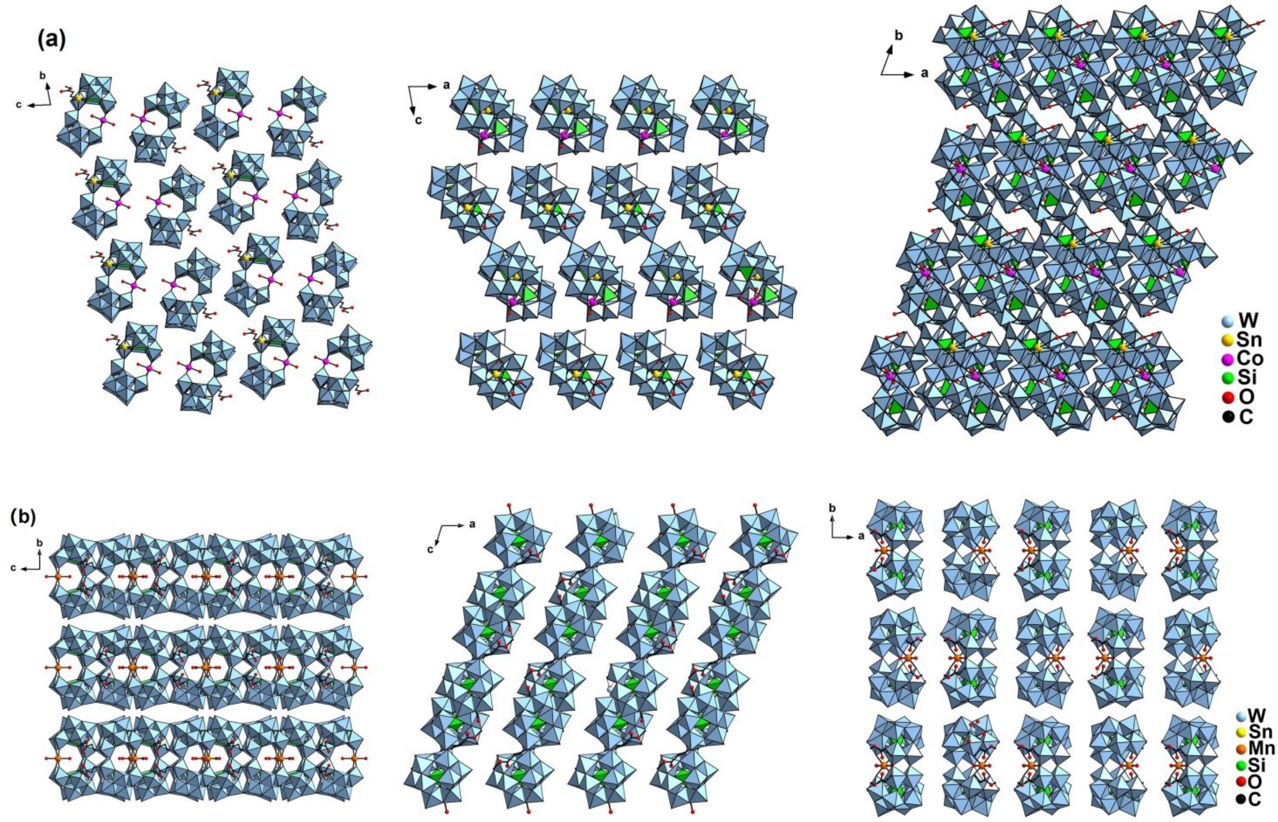

Figure S3 The packing arrangement of the polyoxoanions in $\mathbf{Si_2W_{19}}$**-Co-SnRCOOCH**$_\mathbf{3}$ (a) and $\mathbf{Si_2W_{19}}$**-Mn-SnRCOOCH**$_\mathbf{3}$ (b) along *a*, *b*, *c* axes, respectively (All H, K and Na atoms, the isolated $[C(NH_2)_3]^+$ cations and crystal water molecules existed in the interspaces are omitted for clarity)

3. Selected bond lengths and angles

Table S2 Selected bond lengths (Å) and angles (°) for $\mathbf{Si_2W_{19}}$**-Co-SnRCOOCH**$_\mathbf{3}$

Bond	**Length (Å)**	**Bond**	**Length (Å)**	**Bond**	**Length (Å)**
W1-O19	1.717(12)	W8-O9	1.908(11)	W15-O58	2.338(10)
W1-O10	1.821(10)	W8-O13	1.912(11)	W15-O31	1.945(11)
W1-O13	1.910(10)	W8-O47	1.933(10)	W16-O23	1.703(11)
W1-O37	1.921(10)	W8-O60	2.365(10)	W16-O30	1.883(11)
W1-O2	2.097(10)	W9-O38	1.753(13)	W16-O29	1.896(10)
W1-O11	2.267(11)	W9-O32	1.764(11)	W16-O57	1.917(13)
W2-O40	1.717(11)	W9-O12	1.950(10)	W16-O67	1.935(11)
W2-O45	1.881(10)	W9-O14	1.966(10)	W16-O33	2.316(9)
W2-O37	1.920(11)	W9-O24	2.102(10)	W17-O69	1.721(11)
W2-O17	1.924(11)	W9-O62	2.232(10)	W17-O3	1.894(10)
W2-O30	1.981(10)	W10-O64	1.701(11)	W17-O41	1.912(11)
W2-O11	2.283(9)	W10-O26	1.817(10)	W17-O46	1.912(11)

W3-O35	1.725(11)	W10-O50	1.909(11)	W17-O68	1.921(12)
W3-O2	1.832(10)	W10-O56	1.948(12)	W17-O22	2.376(10)
W3-O29	1.929(10)	W10-O6	1.980(11)	W18-O66	1.709(11)
W3-O47	1.954(10)	W10-O60	2.303(10)	W18-O14	1.884(11)
W3-O56	1.966(12)	W11-O55	1.737(11)	W18-O16	1.889(11)
W3-O60	2.317(10)	W11-O27	1.757(11)	W18-O67	1.921(11)
W4-O53	1.718(12)	W11-O12	1.924(11)	W18-O17	1.937(12)
W4-O1	1.746(11)	W11-O9	1.927(12)	W18-O33	2.365(9)
W4-O41	1.921(10)	W11-O26	2.139(10)	W19-O61	1.716(11)
W4-O43	1.927(11)	W11-O62	2.231(9)	W19-O21	1.835(11)
W4-O25	2.126(12)	W12-O52	1.729(10)	W19-O46	1.962(12)
W4-O5	2.249(11)	W12-O25	1.818(11)	W19-O18	1.964(11)
W5-O51	1.699(12)	W12-O31	1.890(11)	W19-O45	1.973(10)
W5-O4	1.877(10)	W12-O3	1.976(11)	W19-O42	2.323(10)
W5-O18	1.888(10)	W12-O28	1.981(11)	Sn1-O34	2.061(11)
W5-O28	1.902(11)	W12-O22	2.313(10)	Sn1-O21	2.064(10)
W5-O68	1.947(12)	W13-O59	1.717(12)	Sn1-O20	2.075(11)
W5-O22	2.294(10)	W13-O24	1.834(10)	Sn1-O10	2.085(10)
W6-O39	1.737(12)	W13-O50	1.905(11)	Sn1-C1	2.117(19)
W6-O20	1.835(11)	W13-O16	1.956(11)	Sn1-O42	2.184(11)
W6-O8	1.943(11)	W13-O57	1.966(11)	Co1-O32	2.034(11)
W6-O63	1.947(10)	W13-O33	2.322(10)	Co1-O54	2.044(11)
W6-O4	1.949(10)	W14-O36	1.714(11)	Co1-O27	2.070(11)
W6-O58	2.319(11)	W14-O34	1.848(10)	Co1-O1	2.090(10)
W7-O54	1.762(11)	W14-O7	1.887(11)	Co1-O1W	2.100(14)
W7-O49	1.772(11)	W14-O63	1.929(12)	Co1-O2W	2.225(12)
W7-O43	1.916(11)	W14-O48	1.945(11)	C1-C2	1.518(10)
W7-O7	1.933(11)	W14-O58	2.342(10)	C2-C3	1.513(10)
W7-O44	2.110(11)	W15-O15	1.714(11)	O70-C3	1.36(2)
W7-O5	2.249(10)	W15-O44	1.828(12)	O71-C3	1.20(2)
W8-O65	1.691(11)	W15-O48	1.920(11)	O70-C4	1.46(3)
W8-O6	1.908(11)	W15-O8	1.930(12)		
Bond	**Angle (°)**	**Bond**	**Angle (°)**	**Bond**	**Angle (°)**
O19-W1-O11	167.1(4)	O65-W8-O60	175.1(5)	O15-W15-O58	171.9(5)
O10-W1-O2	168.6(5)	O9-W8-O47	156.8(5)	O48-W15-O31	161.2(5)
O2-W1-O11	80.6(4)	O47-W8-O60	76.4(4)	O48-W15-O58	75.5(4)

O37-W1-O11	73.8(4)	O6-W8-O60	76.4(4)	O8-W15-O58	71.0(4)
O40-W2-O11	172.0(5)	O38-W9-O62	169.6(5)	O23-W16-O33	172.3(5)
O45-W2-O30	168.2(4)	O32-W9-O24	166.3(5)	O29-W16-O67	162.4(4)
O37-W2-O11	73.5(4)	O12-W9-O62	74.3(4)	O57-W16-O33	72.6(4)
O30-W2-O11	81.5(4)	O24-W9-O62	80.2(4)	O67-W16-O33	76.2(4)
O35-W3-O60	172.0(4)	O64-W10-O60	170.4(5)	O69-W17-O22	176.1(5)
O29-W3-O47	162.9(4)	O50-W10-O6	162.5(4)	O3-W17-O46	156.0(5)
O47-W3-O60	77.2(4)	O56-W10-O60	72.0(4)	O68-W17-O22	75.0(4)
O56-W3-O60	71.3(4)	O6-W10-O60	76.6(4)	O3-W17-O22	75.5(4)
O53-W4-O5	169.2(5)	O55-W11-O62	168.7(5)	O66-W18-O33	176.8(4)
O1-W4-O25	166.9(5)	O27-W11-O26	166.5(4)	O16-W18-O17	157.1(4)
O43-W4-O5	73.9(4)	O26-W11-O62	79.7(4)	O16-W18-O33	76.3(4)
O25-W4-O5	80.7(4)	O12-W11-O62	74.8(4)	O67-W18-O33	75.3(4)
O51-W5-O22	171.4(5)	O52-W12-O22	168.0(4)	O61-W19-O42	176.5(6)
O4-W5-O68	162.8(5)	O31-W12-O3	160.6(5)	O18-W19-O45	164.9(4)
O28-W5-O22	73.1(4)	O3-W12-O22	75.7(4)	O46-W19-O42	82.9(4)
O68-W5-O22	76.5(4)	O28-W12-O22	71.3(4)	O18-W19-O42	81.9(4)
O63-W6-O4	159.8(5)	O59-W13-O33	170.3(5)	C1-Sn1-O42	174.5(6)
O39-W6-O58	170.6(5)	O50-W13-O16	161.3(5)	O20-Sn1-O10	170.3(4)
O8-W6-O58	71.2(4)	O16-W13-O33	76.1(4)	O21-Sn1-O42	75.5(4)
O63-W6-O58	74.5(4)	O57-W13-O33	71.7(4)	O10-Sn1-O42	85.0(4)
O49-W7-O5	167.9(5)	O36-W14-O58	172.9(5)	O27-Co1-O1	177.1(4)
O54-W7-O44	165.6(5)	O34-W14-O48	158.1(5)	O1W-Co1-O2W	176.9(5)
O43-W7-O5	74.1(4)	O63-W14-O58	74.3(4)	O32-Co1-O1	87.3(4)
O44-W7-O5	79.3(4)	O48-W14-O58	74.9(4)	O32-Co1-O1W	87.0(5)

Table S3 Selected bond lengths (Å) and angles (º) for **Si_2W_{19}-Mn-SnRCOOCH$_3$**

Bond	**Length (Å)**	**Bond**	**Length (Å)**	**Bond**	**Length (Å)**
W1-O11	1.733(8)	W5-O33	1.855(8)	W9-O25	1.897(8)
W1-O35	1.755(7)	W5-O2	1.915(4)	W9-O29	1.905(8)
W1-O4	1.914(7)	W5-O18	1.936(7)	W9-O13	1.910(8)
W1-O12	1.934(7)	W5-O19	1.945(7)	W9-O24	2.359(6)
W1-O6	2.131(7)	W5-O21	2.290(6)	W10-O36	1.69(2)
W1-O31	2.228(7)	W6-O5	1.704(8)	W10-O1	1.944(4)
W2-O23	1.710(7)	W6-O10	1.817(7)	W10-O26	1.984(8)
W2-O8	1.778(7)	W6-O3	1.924(7)	W10-O33	2.011(7)

W2-O25	1.918(8)	W6-O17	1.931(8)	W10-O10	2.108(7)
W2-O4	1.932(8)	W6-O29	1.941(7)	W10-O21	2.183(7)
W2-O32	2.117(7)	W6-O24	2.297(7)	Sn1-O1	1.944(4)
W2-O31	2.246(7)	W7-O15	1.716(8)	Sn1-O26	1.984(8)
W3-O22	1.710(8)	W7-O3	1.871(7)	Sn1-O33	2.011(7)
W3-O32	1.806(8)	W7-O28	1.890(8)	Sn1-C1	2.082(10)
W3-O9	1.923(7)	W7-O19	1.896(7)	Sn1-O10	2.108(7)
W3-O13	1.929(7)	W7-O14	1.952(7)	Sn1-O21	2.183(7)
W3-O17	1.962(8)	W7-O20	2.310(7)	Mn1-O8	2.102(7)
W3-O24	2.321(7)	W8-O34	1.703(7)	Mn1-O35	2.148(7)
W4-O7	1.720(8)	W8-O16	1.887(8)	Mn1-O1W	2.209(11)
W4-O6	1.791(7)	W8-O12	1.887(8)	Mn1-O2W	2.254(11)
W4-O9	1.889(7)	W8-O18	1.901(7)	O37-C3	1.11(3)
W4-O16	1.968(7)	W8-O14	1.908(8)	O38-C3	1.31(3)
W4-O28	1.994(8)	W8-O20	2.363(7)	O38-C4	1.464(10)
W4-O20	2.313(7)	W9-O30	1.701(7)	C1-C2	1.511(10)
W5-O27	1.709(7)	W9-O26	1.866(8)	C2-C3	1.499(10)
Bond	**Angle (°)**	**Bond**	**Angle (°)**	**Bond**	**Angle (°)**
O11-W1-O31	168.3(3)	O27-W5-O21	174.8(3)	O30-W9-O24	175.5(3)
O35-W1-O6	167.8(3)	O2-W5-O19	167.5(4)	O26-W9-O13	156.8(3)
O6-W1-O31	80.6(3)	O33-W5-O21	75.1(3)	O29-W9-O24	75.2(3)
O12-W1-O6	82.9(3)	O18-W5-O21	82.7(3)	O13-W9-O24	75.9(3)
O23-W2-O31	167.0(3)	O5-W6-O24	171.4(3)	O36-W10-O21	168.4(10)
O8-W2-O32	166.4(3)	O3-W6-O29	161.6(3)	O1-W10-O10	169.6(4)
O4-W2-O31	74.0(3)	O17-W6-O24	72.4(3)	O33-W10-O21	74.7(3)
O32-W2-O31	79.2(3)	O29-W6-O24	76.1(3)	O10-W10-O21	82.5(3)
O22-W3-O24	171.6(3)	O15-W7-O20	172.2(4)	C1-Sn1-O21	172.0(18)
O9-W3-O13	161.5(3)	O3-W7-O14	161.2(3)	O1-Sn1-O10	169.6(4)
O13-W3-O24	76.6(3)	O14-W7-O20	76.3(3)	O33-Sn1-O21	74.7(3)
O17-W3-O24	71.3(3)	O28-W7-O20	73.9(3)	O10-Sn1-O21	82.5(3)
O7-W4-O20	169.1(3)	O34-W8-O20	176.3(3)	O1W-Mn1-O2W	178.1(5)
O9-W4-O16	160.1(3)	O16-W8-O18	156.7(3)	O8-Mn1-O35#1	172.0(3)
O16-W4-O20	76.1(3)	O14-W8-O20	75.8(3)	O35#1-Mn1-O35	84.0(4)
O28-W4-O20	72.1(3)	O16-W8-O20	76.3(3)	O8#1-Mn1-O1W	87.0(3)

Symmetry transformations used to generate equivalent atoms: #1 x,-y+1,z

Table S4 Hydrogen bonds for **Si_2W_{19}-Co-SnRCOOCH$_3$**

D–H...A	d(D–H) (Å)	d(H...A) (Å)	d(D...A) (Å)	<(DHA) (°)
N1-H1A...O24	0.86	2.21	2.972(18)	148.2
N1-H1A...O26	0.86	2.40	3.00(2)	127.5
N1-H1B...O51#8	0.86	2.05	2.896(18)	168.8
N2-H2A...O24	0.86	2.29	3.035(19)	145.3
N2-H2A...O38	0.86	2.47	3.163(19)	137.8
N2-H2B...O63#6	0.86	2.02	2.86(2)	165.6
N3-H3A...O36#6	0.86	2.15	2.991(19)	166.0
N3-H3B...O68#8	0.86	2.02	2.872(17)	170.8
N4-H4A...O65#9	0.86	2.18	3.02(2)	163.6
N5-H5A...O2#3	0.86	2.46	3.206(19)	145.8
N5-H5A...O30#3	0.86	2.27	2.915(19)	131.4
N5-H5A...O37#3	0.86	2.47	3.142(18)	135.6
N5-H5B...O40	0.86	2.17	2.983(19)	157.3
N6-H6A...O2#3	0.86	2.46	3.21(2)	146.4
N6-H6A...O19#3	0.86	2.56	3.28(2)	142.5
N6-H6B...O47#9	0.86	2.06	2.91(2)	172.3
N7-H7A...O52#1	0.86	2.08	2.924(19)	168.4
N7-H7B...O44	0.86	2.08	2.894(18)	157.9
N8-H8A...O12#4	0.86	2.23	3.038(19)	156.5
N8-H8B...O49	0.86	2.14	2.98(2)	167.6
N9-H9A...O28#1	0.86	2.13	2.986(19)	172.0
N9-H9B...O12#4	0.86	2.52	3.266(19)	146.4
N9-H9B...N1#4	0.86	2.61	3.20(2)	126.4
N10-H10A...O31#1	0.86	2.40	3.18(2)	150.9
N10-H10B...O25	0.86	2.27	3.08(2)	156.8
N11-H11A...O55#4	0.86	2.27	3.05(3)	159.6
N11-H11B...O53	0.86	2.46	3.22(3)	147.7
N12-H12A...O14W#1	0.86	2.34	3.12(3)	150.9
N12-H12B...O4#1	0.86	2.58	3.20(2)	130.0
N12-H12B...O8#1	0.86	2.51	3.29(2)	151.1
N13-H13A...O46	0.86	2.65	3.30(2)	133.2
N13-H13A...O61	0.86	2.13	2.93(2)	153.9
N13-H13B...O4W#9	0.86	2.34	3.09(3)	145.6
N14-H14A...O29#3	0.86	2.56	3.30(2)	144.6

N14-H14A...O35#3	0.86	2.45	3.21(2)	147.4
N14-H14B...O23#3	0.86	2.51	3.06(2)	122.0
N14-H14B...O61	0.86	2.38	3.12(2)	145.6
N15-H15A...O19#9	0.86	2.51	3.00(2)	117.7
N15-H15A...O35#3	0.86	2.31	3.10(3)	152.4
N15-H15B...O4W#9	0.86	2.20	2.99(3)	151.7

Symmetry transformations used to generate equivalent atoms: #1 -x+1,-y+1,-z+1; #2 -x+2,-y+1,-z+1 #3 -x+1,-y,-z+2; #4 -x+2,-y,-z+1; #5 x,y+1,z; #6 x,y-1,z; #7 x-1,y+1,z; #8 x+1,y-1,z; #9 x-1,y,z

Table S5 Hydrogen bonds for Si_2W_{19}-Mn-SnRCOOCH$_3$

D–H...A	d(D–H) (Å)	d(H...A) (Å)	d(D...A) (Å)	<(DHA) (°)
N1–H1A...O5#4	0.86	2.65	3.098(15)	113.4
N1–H1B...O3	0.86	2.61	3.241(14)	131.6
N1–H1B...O9	0.86	2.61	3.333(15)	141.9
N1–H1B...O17	0.86	2.37	3.105(15)	143.8
N2–H2A...O6#3	0.86	2.23	3.054(14)	161.1
N2–H2B...O9	0.86	2.30	3.090(14)	153.7
N3–H3A...O11#3	0.86	2.18	2.968(18)	151.6
N4–H4A...O7	0.86	2.11	2.938(15)	161.5
N4–H4B...O32#3	0.86	2.11	2.926(16)	157.4
N5–H5B...O8W	0.86	2.20	3.02(4)	157.6
N5–H5B...O8W#2	0.86	2.52	3.29(4)	149.9
N5–H5A...O28	0.86	2.09	2.946(15)	174.6
N6–H6A...O23#3	0.86	2.18	3.034(19)	173.8
N7–H7A...O8#5	0.86	2.10	2.938(13)	164.6
N7–H7B...O25#1	0.86	2.33	3.097(14)	149.2
N7–H7B...O30#1	0.86	2.58	3.259(15)	137.1
N8–H8A...O26#1	0.860(10)	2.29(3)	3.145(15)	171(16)

Symmetry transformations used to generate equivalent atoms: #1 x,-y+1,z; #2 -x,y,-z-1; #3 -x+1/2,-y+1/2,-z; #4 -x+1/2,-y+1/2,-z-1; #5 -x+1,-y+1,-z

4. Chemical and physical characterizations

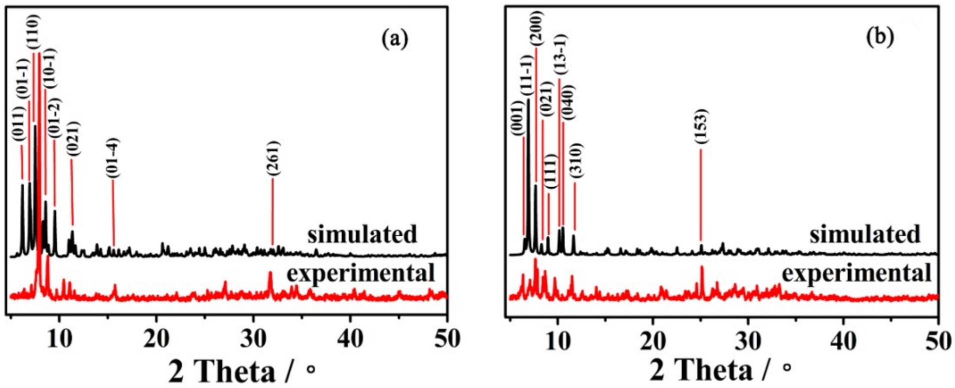

Figure S4 The simulated and experimental XRPD patterns of **Si_2W_{19}-Co-$SnRCOOCH_3$** (a) and **Si_2W_{19}-Mn-$SnRCOOCH_3$** (b)

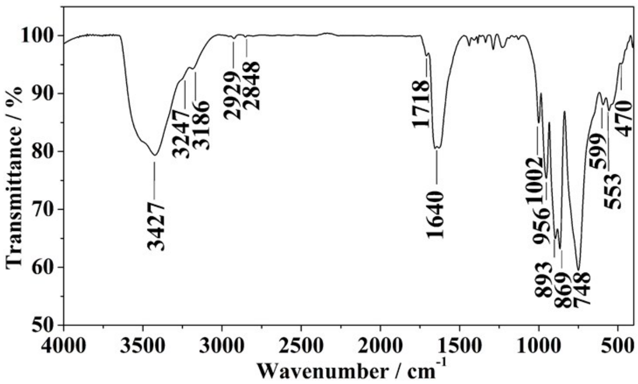

Figure S5 The IR spectrum of **Si_2W_{19}-Co-$SnRCOOCH_3$**

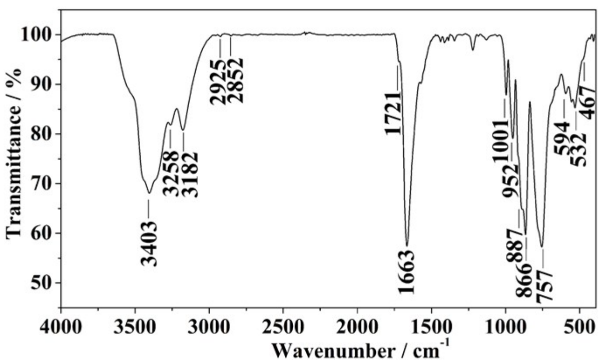

Figure S6 The IR spectrum of **Si_2W_{19}-Mn-$SnRCOOCH_3$**

As shown in Figures S5 and S6, compounds **Si_2W_{19}-Co-$SnRCOOCH_3$** and **Si_2W_{19}-Mn-$SnRCOOCH_3$** have similar IR spectra. Take **Si_2W_{19}-Co-$SnRCOOCH_3$** for example, the peaks at 2929 and 2848 cm^{-1} are attributed to the organic group $-CH_2$, and the v(N–H) peaks lie in the 3247–3186 cm^{-1} region.[S1] The $\nu_{as}(COO^-)$ vibration and $v_s(COO^-)$ appears at 1718–1640 cm^{-1}. The peaks at 1002, 956, 893(sh), 869 and 748 cm^{-1} can be ascribed to the characteristic vibrations of $v_{as}(Si–O_a)$, $v_{as}(W=O_d)$, $v(W/Sn–O_b)$, and $v(W–O_c)$ of POMs,[S2,S3] respectively (O_a and O_d represent tetrahedral and terminal O atoms, and O_b and O_c represent corner-sharing and edge-sharing O atoms). The characteristic W/Sn–O_b asymmetric stretching vibration splits into two peaks (893 and 869 cm^{-1}), which suggests that the POM subunits have a typical bivacant asymmetric structures.[S4] The appearance of a peak at 470 cm^{-1} is assigned to the stretching vibration of Sn–O bond. Peaks at 553 cm^{-1} and 599 cm^{-1} may be due to the antisymmetric and symmetric vibration peaks of Sn−C bond.[S5] A peak at 3427 cm^{-1} is assigned to be lattice water molecules. All the results indicate the presence of the estertin group and the POM framework in compounds **Si_2W_{19}-Co-SnRCOOCH$_3$** and **Si_2W_{19}-Mn-SnRCOOCH$_3$**, which are in good agreement with the single crystal structural analysis.

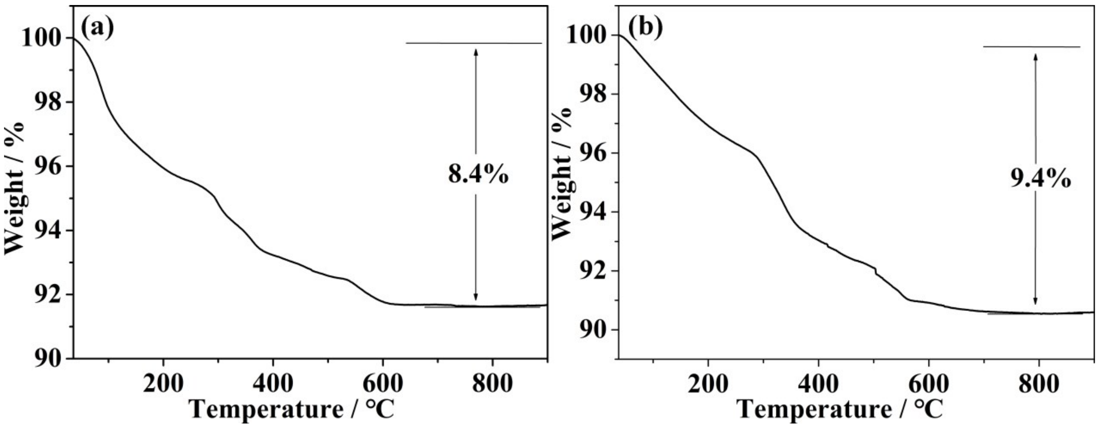

Figure S7 TG curves of **Si_2W_{19}-Co-SnRCOOCH$_3$** (a) and **Si_2W_{19}-Mn-SnRCOOCH$_3$** (b)

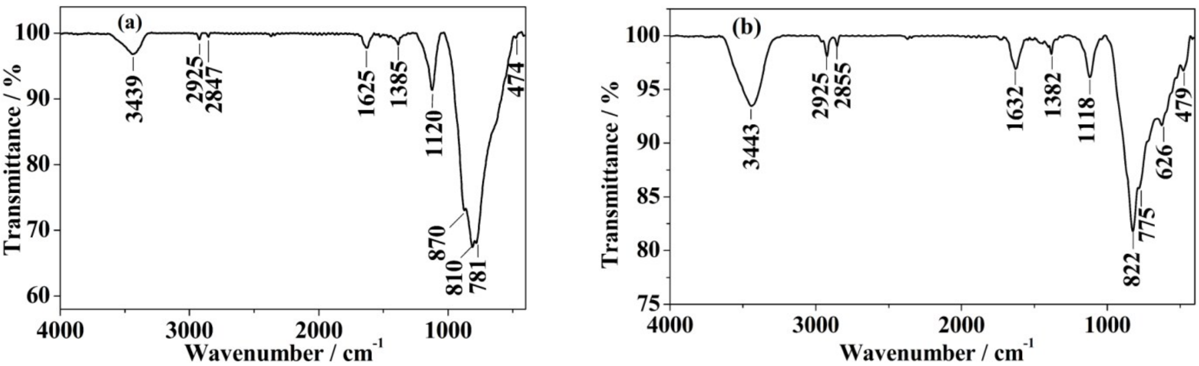

Figure S8 IR spectra of **Si_2W_{19}-Co-SnRCOOCH$_3$** (a) and **Si_2W_{19}-Mn-SnRCOOCH$_3$** (b) after heating at 800 °C in air

As seen from the IR spectra of **Si_2W_{19}-Co-SnRCOOCH$_3$** (a) and **Si_2W_{19}-Mn-SnRCOOCH$_3$** (b) displayed in Figure S8, the characteristic peaks of –CH_2 and −COO at 2925−2855 cm^{-1} and 1632−1382 cm^{-1} respectively still remained, and the peaks of Sn−O at 479−474 cm^{-1} and the peak of Sn−C at about 626 cm^{-1} also can be seen, and the characteristic vibrations of POMs within 775-1120 cm^{-1} still exist, indicating that the introduction of TM and OM enhances the stability of the two POM anions.

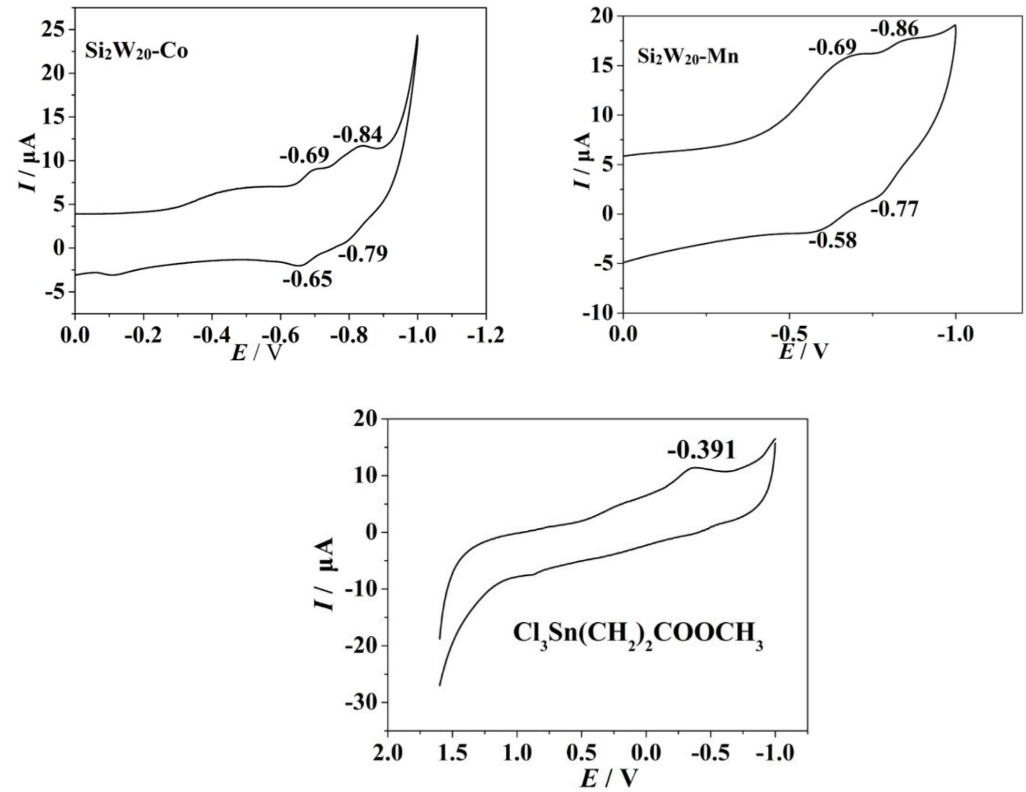

Figure S9 CV curves of **Si_2W_{20}-Co**, **Si_2W_{20}-Mn** and $Cl_3Sn(CH_2)_2COOCH_3$ in 0.4 mol L^{-1} NaAc-HAc (pH = 4.8) buffer solution at the scan rate of 50 mV s^{-1}

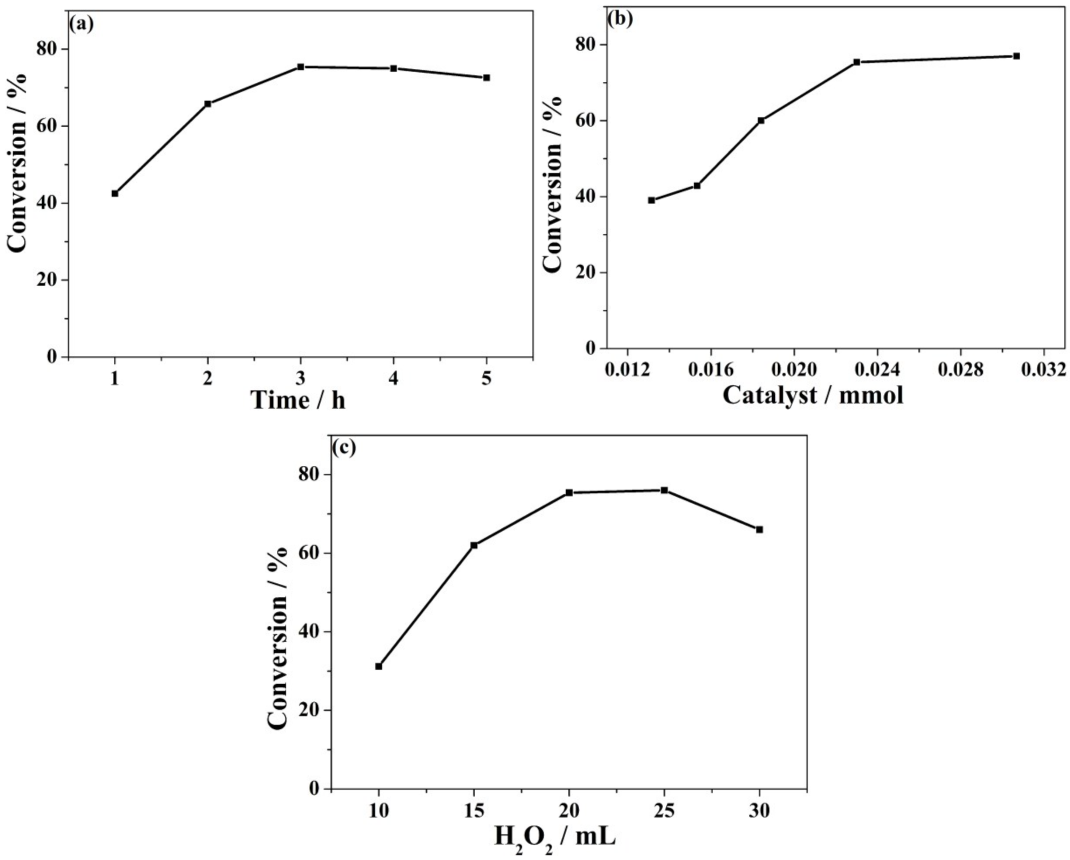

Figure S10 Effect of reaction time (a), the amount of **Si_2W_{20}-Co** (b) and H_2O_2 (c) on cyclohexanone conversion

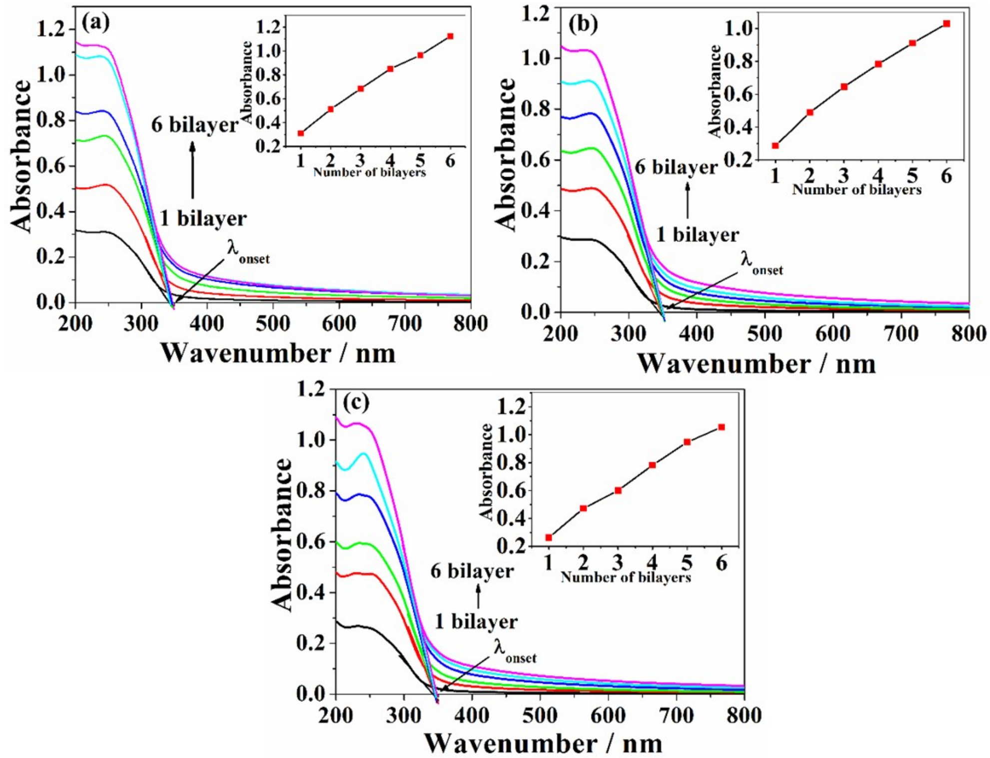

Figure S11 UV-vis absorption spectra of multilayer films (**Si_2W_{19}-Co-$SnRCOOCH_3$**/TiO_2)$_n$ (a), (**Si_2W_{19}-Mn-$SnRCOOCH_3$**/TiO_2)$_n$ (b) and (PSS/TiO_2)$_n$ (c) on quartz substrates with n= 1−6 . (Inset) Relationship of absorbance at 242 nm *vs* the number of layers

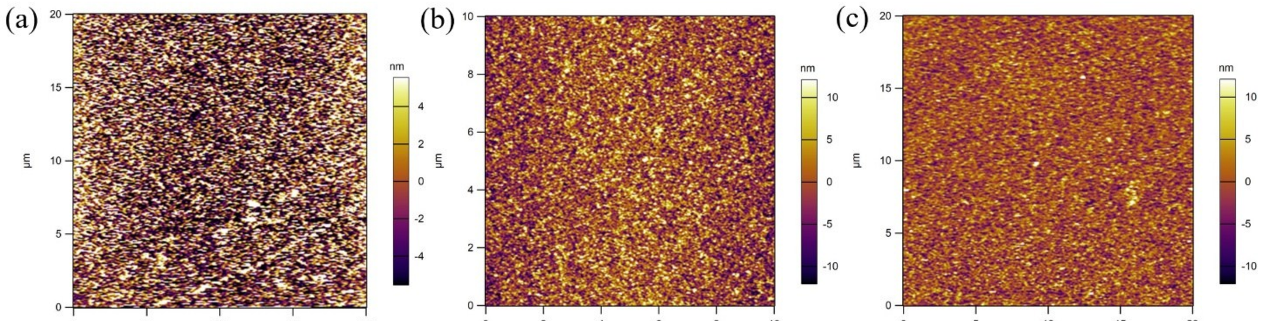

Figure S12 AFM images of (**Si_2W_{19}-Co-$SnRCOOCH_3$**/TiO_2)$_4$ (a), (**Si_2W_{19}-Mn-$SnRCOOCH_3$**/TiO_2)$_4$ (b) and (PSS/TiO_2)$_4$ (c) films assembled on silicon substrate

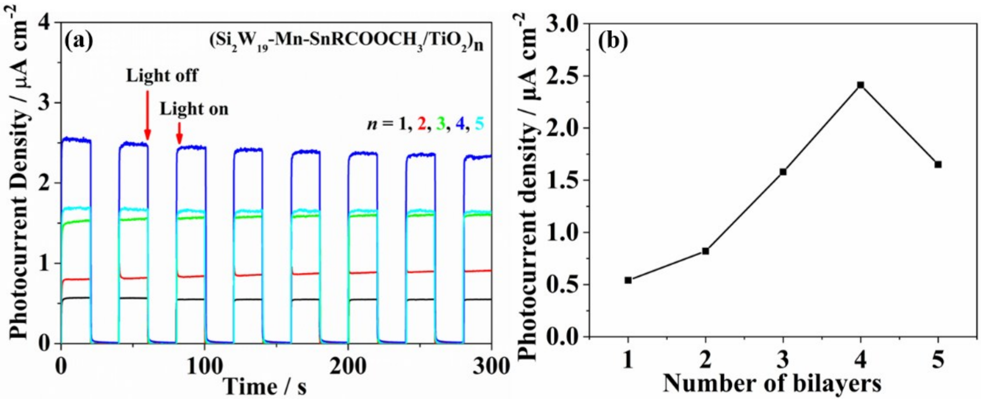

Figure S13 Periodic on/off photocurrent response of (**Si_2W_{19}-Mn-SnRCOOCH$_3$**/TiO$_2$)$_n$ films (n = 1−5) recorded in 0.1 mol L^{-1} Na_2SO_4 at a bias of 0 V *vs*. Ag/AgCl (a), relationship of the photocurrent *vs*. the number of bilayers (b)

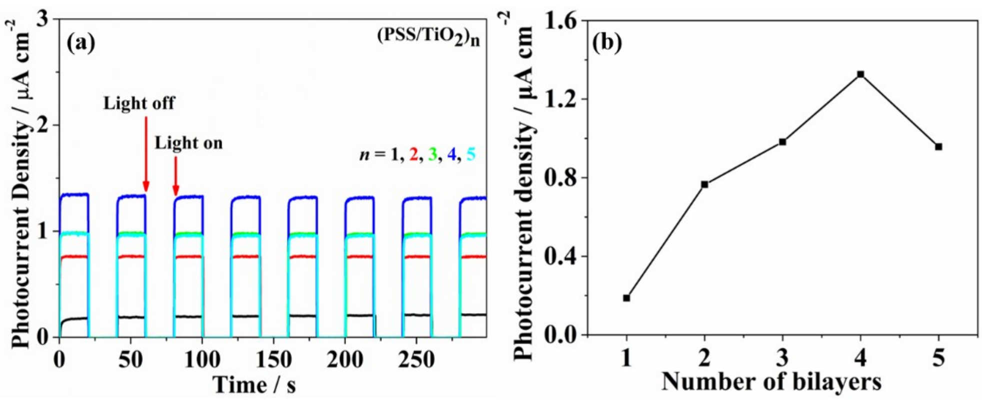

Figure S14 Periodic on/off photocurrent response of (PSS/TiO$_2$)$_n$ films (n = 1−5) recorded in 0.1 mol L^{-1} Na_2SO_4 at a bias of 0 V *vs*. Ag/AgCl (a), relationship of the photocurrent *vs*. the number of bilayers (b)

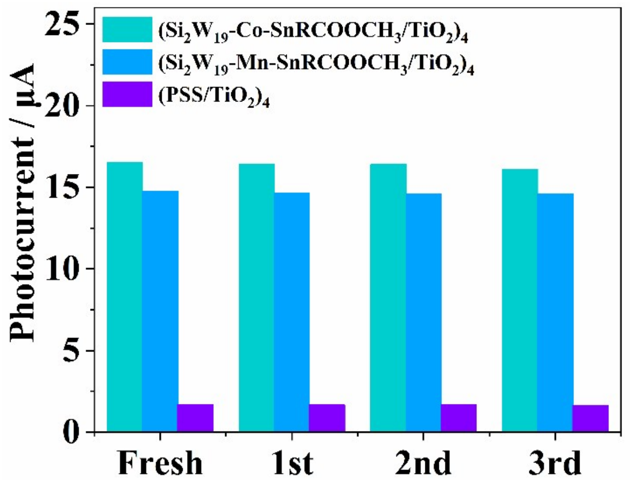

Figure S15 The recycle of (**Si_2W_{19}-Co-SnRCOOCH$_3$**/TiO$_2$)$_4$, (**Si_2W_{19}-Mn-SnRCOOCH$_3$**/TiO$_2$)$_4$ and (PSS/TiO$_2$)$_4$ composite films in photoelectrocatalysis in 0.5 mol L^{-1} methanol

Table S6 The redox potentials of frontier molecular orbitals of **Si_2W_{19}-Co-SnRCOOCH$_3$** (TM = Mn, Co) and TiO_2

	LUMO/CB (*vs*. NHE)	HOMO/VB (*vs*. NHE)
Si_2W_{19}-Co-SnRCOOCH$_3^-$	−0.41 V	3.45 V
Si_2W_{19}-Mn-SnRCOOCH$_3$	−0.42 V	3.5 V
TiO_2	−0.5 V	2.7 V

References

[S1] Junwei Zhao, Jie Zhang, You Song, Shoutian Zheng, Guoyu Yang. Two hexanickel-substituted Keggin-type germanotungstates. Eur. J. Inorg. Chem., 2008, 2008(24): 3809–3819.

[S2] Lubin Ni, Firasat Hussain, Bernhard Spingler, Stephen Weyeneth, Greta R. Patzke. Lanthanoid-containing open Wells-Dawson silicotungstates: synthesis, crystal structuers, and properties. Inorg. Chem., 2011, 50(11): 4944–4955.

[S3] Ke Wang, Pengtao Ma, Qingxia Yan, Jingping Wang, Jingyang Niu. A novel flower basket-shaped organosilyl derivative based on trivacant tungstosilicate: $[(C_4H_9)_4N]_3H[\alpha\text{-A-}SiW_9O_{34}(CH_3SiO)_6] \cdot 3H_2O$. Inorg. Chem. Commun., 2011, 14(9): 1377–1380.

[S4] Jingping Wang, Junwei Zhao, Xianying Duan,, Jingyang Niu. Syntheses and strutures of one- and two-dimensional organic-inorganic hybrid rare earth derivatives based on monovacant Keggin-type polyoxotungstates. Cryst. Growth Des., 2006, 6(2): 507–513.

[S5] M. Khawar Rauf, M. Adeel Saeed, Ud Din Imtiaz, M. Bolte, A. Badshah, B. Mirza. Synthesis, characterization and biological activities of some new organotin(IV) derivatives: crystal struvture of $[(SnPh_3)(OOCC_6H_4OH)]$ and $[(SnMe_3)_2(OOC)_2C_6Cl_4(DMSO)_2]$. J. Organomet. Chem., 2008, 693(18): 3043–3048.